Chemosphere 138 (2015) 218–224

Contents lists available at ScienceDirect

Chemosphere

journal homepage: www.elsevier.com/locate/chemosphere

# Effects of natural organic matter on calcium and phosphorus co-precipitation

Hugo R. Sindelar *, Mark T. Brown, Treavor H. Boyer *

*Department of Environmental Engineering Sciences, University of Florida, P.O. Box 116450, Gainesville, FL 32611-6450, USA*

## HIGHLIGHTS

- Dissolved organic carbon inhibits calcium and phosphorus co-precipitation.
- Dissolved organic carbon and phosphorus can co-precipitate with calcium at high pH.
- Aromatic dissolved organic carbon preferentially inhibits calcium precipitation.
- Phosphorus density on calcite is higher with increased dissolved organic carbon.
- High pH sites promote phosphorus co-precipitation with calcite in natural systems.

## GRAPHICAL ABSTRACT

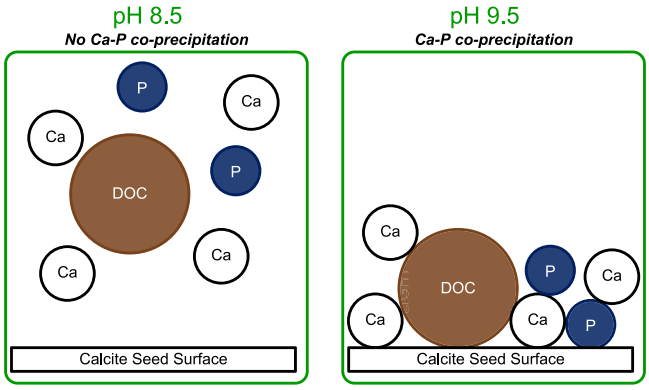


## ARTICLE INFO

*Article history:*
Received 2 June 2014
Received in revised form 26 April 2015
Accepted 3 May 2015

*Keywords:*
Calcium
Phosphorus
Natural organic matter
Co-precipitation

## ABSTRACT

Phosphorus (P), calcium (Ca) and natural organic matter (NOM) naturally occur in all aquatic ecosystems. However, excessive P loads can cause eutrophic or hyper-eutrophic conditions in these waters. As a result, P regulation is important for these impaired aquatic systems, and Ca–P co-precipitation is a vital mechanism of natural P removal in many alkaline systems, such as the Florida Everglades. The interaction of P, Ca, and NOM is also an important factor in lime softening and corrosion control, both critical processes of drinking water treatment. Determining the role of NOM in Ca–P co-precipitation is important for identifying mechanisms that may limit P removal in both natural and engineered systems. The main goal of this research is to assess the role of NOM in inhibiting Ca and P co-precipitation by: (1) measuring how Ca, NOM, and P concentrations affect NOM's potential inhibition of co-precipitation; (2) determining the effect of pH; and (3) evaluating the precipitated solids. Results showed that Ca–P co-precipitation occurs at pH 9.5 in the presence of high natural organic matter (NOM) (≈30 mg $L^{-1}$). The supersaturation of calcite overcomes the inhibitory effect of NOM seen at lower pH values. Higher initial P concentrations lead to both higher P precipitation rates and densities of P on the calcite surface. The maximum surface density of co-precipitated P on the precipitated calcite surface increases with increasing NOM levels, suggesting that NOM does prevent the co-precipitation of Ca and P.



* Corresponding authors at: 1612 S 3rd Ave., Bozeman, MT 59715, USA.
*E-mail addresses:* hugo.sindelar@msu.montana.edu (H.R. Sindelar), thboyer@ufl.edu (T.H. Boyer).

http://dx.doi.org/10.1016/j.chemosphere.2015.05.008
0045-6535/

## 1. Introduction

Phosphorus (P), calcium (Ca) and natural organic matter (NOM) play an important role in both surface waters and drinking water treatment systems. P, Ca, and NOM (measured as dissolved organic carbon (DOC)) naturally occur in every aquatic ecosystem; however, excessive P loads can cause eutrophic or hyper-eutrophic conditions in surface waters. These conditions are characterized by excessive primary productivity, reduction or depletion of dissolved oxygen, stressed aquatic organisms, and simplified trophic structure. P regulation is critical for many aquatic systems, and P co-precipitation with Ca, referred to as Ca–P co-precipitation in this study, is an important mechanism of natural P removal. Studies have shown, however, that DOC concentrations as low as 2.5 mg C $L^{-1}$ can inhibit Ca precipitation and significantly reduce calcite ($CaCO_3$) growth (Hoch et al., 2000; Lin et al., 2005). Thus, DOC may negatively affect removal of P in natural systems by inhibiting Ca–P co-precipitation, but more research is necessary to assess the extent of this effect. Determining the role of DOC in Ca–P co-precipitation is important for identifying mechanisms that may limit P removal in natural and engineered systems where high P levels are a concern.

The interaction of P, Ca, and DOC is also relevant for water treatment and distribution systems. P is often introduced during water treatment processes for corrosion control and enhancement of biofiltration processes (Lauderdale et al., 2012). Ca is introduced during water treatment for lime softening, and DOC is a natural component of the raw water. The interactions of P, Ca, and DOC have significant implications for the effectiveness of corrosion control processes, biofiltration, and lime softening.

P and DOC both compete for active crystal growth sites with the free calcium ion, $Ca^{2+}$, leading to lower calcite precipitation rates, which has the potential to hinder the softening process (Lin et al., 2005; Lin and Singer, 2006). P is also used for nutrient enrichment of biofiltration process that remove DOC (Lauderdale et al., 2012). As a result, the potential interactions of P, Ca, and DOC will be important for this emerging technology.

Corrosion studies have pointed to complex reactions between P, Ca, and DOC. The potential interactions of P with Ca and DOC can cause both positive and negative effects on corrosion control. For example, the formation of apatites (a group of calcium phosphorus minerals) can reduce corrosion in copper distribution systems; however, phosphate use in copper pipes can also decrease the formation of a protective malachite layer (Dartmann et al., 2004). DOC in the water may affect the performance of scale formation by decreasing the formation of Ca–P complexes, which may or may not be beneficial to corrosion control depending on the inhibitor used, the DOC concentration, and the material in the distribution system. An improved understanding of how P, Ca, and DOC interact will help water treatment professionals design and operate systems with better efficiency and reduced corrosion.

Previous work on P, Ca, and DOC has focused solely on the interactions between two of these three constituents. Studies have evaluated DOC and Ca, and their results show that DOC can significantly inhibit Ca precipitation in natural and engineered systems (Hoch et al., 2000; Lin et al., 2005). Other studies have looked at the importance of Ca–P co-precipitation to P removal in natural waters. Diaz et al. (1994) showed large decreases in aqueous P concentrations in response to pH and calcium increases. However, to the authors' knowledge, no work has been completed on all three of these water chemistry parameters at the same time. Simultaneous evaluation of P, Ca, and DOC is needed to determine how DOC affects Ca–P co-precipitation, thus enabling a better understanding of P removal by precipitation in both engineered and natural systems.

The main goal of this research is to assess the role of DOC in Ca and P co-precipitation. The specific objectives are to: (1) measure how the DOC concentration affects Ca–P co-precipitation, (2) compare the effect of differing pH values on Ca–P co-precipitation in the presence of DOC, (3) determine the types of minerals precipitated, and (4) evaluate whether DOC co-precipitates with either Ca or P during calcite precipitation.

## 2. Materials and methods

### 2.1. pH-stat apparatus

A pH-stat system was used to study the effect of DOC and P concentration on Ca–P co-precipitation rates. Tomson and Nancollas (1978) introduced the pH-stat system, which creates a constant degree of supersaturation relative to a solid phase by maintaining solution pH and composition. All experiments were conducted in a 600 mL jacketed beaker (Ace Glass, Inc.) The jacket contained circulating water from a temperature controlled water bath that insured all experiments were conducted at 25 °C. For this study, Acros Organics 99+% ACS reagent calcite seed crystals ($CaCO_3$), purchased from Fisher Scientific (Cat. No. AC423511000), were introduced as a dry-powder into an experimental solution (see Section 2.2) with equimolar Ca and $CO_3$ concentrations, which caused the precipitation of calcite and decreased the solution pH. The specific surface area of the calcite seed was 0.323 $m^2\ g^{-1}$ as determined by a six-point $N_2$-BET method (Brunauer et al., 1938). The experimental solutions were stirred at a rate sufficient for good mixing. Equal volumes of 0.053 M ($I$ = 0.1 M) $CaCl_2$ and $Na_2CO_3$ titrant solutions were added using a syringe pump (Harvard Apparatus 22) to return the pH to the set value (either 8.5 or 9.5), and maintain the constant degree of supersaturation. These titrant solutions were based on concentrations in previous research used to estimate calcium precipitation in the presence of NOM (Hoch et al., 2000; Lin et al., 2005). The titrant solutions are not the same as the experimental solutions (see Section 2.2), which were added to the jacketed beaker before the addition of the calcite seed. The syringe pump was controlled using a PHCN-37 pH controller (Omega Engineering) with a Thermo Fisher Orion 9156BNWP electrode to maintain solution pH. The pH controller maintained pH within ±0.05 pH units of the set value. The pH controller was calibrated daily with pH 7 and 10 standards (Fisher Scientific). A datalogger (CR510, Campbell Scientific) was used to continuously record pH, time, and titrant volume added.

The amount of titrant used to maintain solution pH and the mass of added calcite seeds were used to calculate the amount of solid precipitated based on the following equation (Hoch et al., 2000; Lin et al., 2005):

$$\text{Ca Precipitation Rate} = \frac{S \times m}{G \times SA} \quad (1)$$

where $S$ is slope (L $s^{-1}$); $m$ is the molarity of the titrant solution (μmol $L^{-1}$); $G$ is the mass of the calcite seed (g); $SA$ is the surface area of the calcite seed ($m^2\ g^{-1}$); and Ca precipitation rates is in the units of μmol $s^{-1}\ m^{-2}$. Ca precipitation rates can be compared across experiments to determine the effect of different DOC and P concentrations on calcite precipitation.

### 2.2. Experimental solutions

Table 1 shows the composition of all reactor experimental solutions used in this study. A range of experimental times were used to allow the calculation of a single Ca and P precipitation rate (see Fig. 1) for each experiment shown in Table 1. The Ca precipitation

**Table 1**
Experimental matrix[a].

| Synthetic water number | pH | P ($\mu g\ P\ L^{-1}$) | DOC[b] ($mg\ C\ L^{-1}$) | Calcite seed (mg) | Experimental time[c] (min) |
|---|---|---|---|---|---|
| 1 | 8.5 | 100 | 0 | 100 | 0, 20, 40, 60, 80, 100[d] |
| 2 | 8.5 | 50 | 0 | 100 | 0, 20, 40, 60, 80, 100[d] |
| 3 | 8.5 | 100 | 0.5 | 100 | 100[d] |
| 4 | 8.5 | 50 | 0.5 | 100 | 100[d] |
| 5 | 8.5 | 100 | 2.5 | 100 | 100[d] |
| 6 | 8.5 | 50 | 2.5 | 100 | 100[d] |
| 7 | 9.5 | 100 | 2.5 | 50 | 0, 7.7 (0.54), 19.9 (0.87), 31.2 (1.25), 41.5 (1.98)[e] |
| 8 | 9.5 | 50 | 2.5 | 50 | 0, 6.6 (0.49), 16.4 (0.05), 26.2 (0.81), 37.3 (0.54)[e] |
| 9 | 9.5 | 100 | 7.5 | 100 | 0, 10.2 (1.32), 33.5 (2.91), 62.8 (7.29), 71.8 (6.88)[e] |
| 10 | 9.5 | 50 | 7.5 | 100 | 0, 7.0 (0.83), 23.3 (1.19), 34.4 (1.80), 49.5 (1.60)[e] |
| 11 | 9.5 | 100 | 15 | 175 | –[f] |
| 12 | 9.5 | 50 | 15 | 175 | 0, 8.5 (1.1), 40.7 (2.4), 66.8 (5.30), 85.8 (4.90)[e] |

[a] For all experiments, reactor Ca concentration was 0.0025 M (prepared using $CaCl_2{\cdot}2H_2O$), carbonate concentration was 0.0025 M (prepared using $NaHCO_3$), and potassium nitrate concentration was 0.094 M (added to maintain the ionic strength of the reactor solution at 0.1 M).
[b] Prepared using Suwannee River NOM (IHSS).
[c] All experiments were repeated in triplicate.
[d] Experimental time in minutes.
[e] Experimental time in minutes with standard deviation in parentheses. Variable pump cycles caused different experimental lengths.
[f] No experiments completed.

rate was calculated using the amount of titrant added to the pH-stat system to maintain constant supersaturation with respect to calcite. The P precipitation rate (see Fig. 1) was calculated for each experimental solution using first-order kinetics and the change in measured P concentration at increasing reaction times (see Supplementary Material). Experiments were conducted in triplicate and the average of triplicate experiments was used to calculate both Ca and P precipitation rates. Experimental times were based on a fixed number of minutes for experiments at a pH of 8.5 and were based on the number of pump cycles at a pH of 9.5. As a result, the experimental times shown in Table 1 for experiments conducted at a pH of 9.5 are average values. No data are shown for experimental solution 11 because of poor repeatability (see Section 3.2).

ACS reagent grade chemicals (Fisher Scientific) and DI water were used for preparation of all experimental solutions. Stock Ca and carbonate solutions were prepared in volumetric flasks using deionized water and calcium chloride dihydrate ($CaCl_2{\cdot}2H_2O$), sodium bicarbonate ($NaHCO_3$), and potassium nitrate ($KNO_3$) to adjust ionic strength to 0.1 M. P was added as monopotassium phosphate ($KH_2PO_4$) from a 100 $mg\ P\ L^{-1}$ stock solution. DOC was added as Suwannee River (SR) NOM (IHSS catalogue number 1R101N). DOC was added to experimental solutions from a 104 $mg\ C\ L^{-1}$ stock solution created by dissolving SRNOM in DI water for 4 h. Stock solutions were not filtered prior to use.

The elemental composition of SR NOM is 7.0% ash, 52.47% C, 4.19% H, 42.69% O, 1.10% N, 0.65% S, and 0.02% P (International Humic Substances Society). It should be noted that the DOC concentrations presented in Table 1 and hereafter are the theoretically calculated values. The measured values were lower with a difference of 25–29%. Two plausible reasons for this discrepancy are: (1) some SRNOM was lost during filtration prior to analysis and/or (2) incomplete dissolution of the SRNOM. However, the authors acknowledge that neither reason can be verified at this time.

Metastable experimental solutions were created by slowly adding an equal volume of stock Ca solution to the stock carbonate solution. P and DOC were then added from each respective stock solution. The total experimental solution volume in the reactor for all experiments was 400 mL, but the volume of each solution

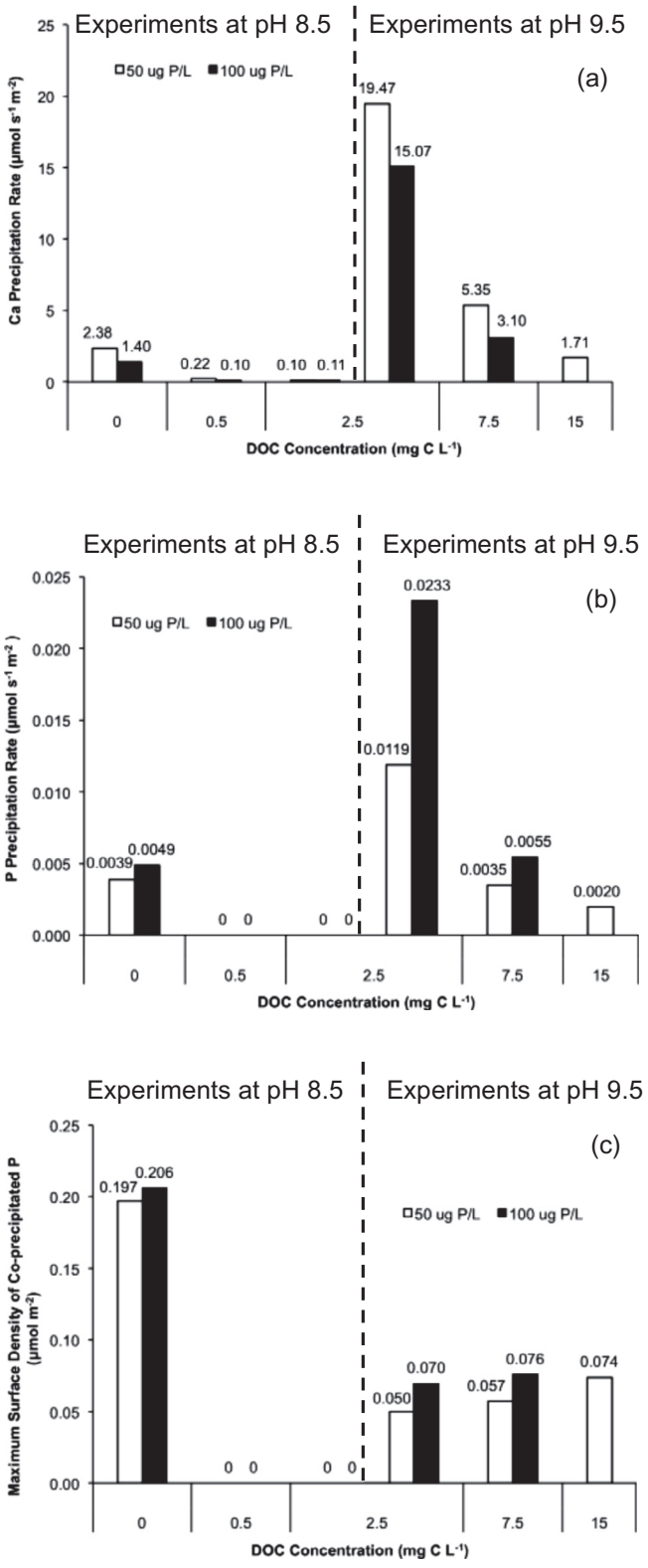


**Fig. 1.** The effect of P, DOC and pH on: Ca precipitation rates (a), P precipitation rates (b), and density of co-precipitated P on the calcite surface (c). For (a) and (b) each bar represents an average precipitation rate calculated based on experiments conducted in triplicate for the different durations listed in Table 1. These rates were normalized to the calcite seed area.

added was dependent on the desired concentrations of both P and DOC. More information about the preparation of experimental solutions is provided in the Supplementary Material. The starting pH, either 8.5 or 9.5, for each experiment was adjusted using 0.1 and 0.01 M NaOH. Metastability was verified by observing constant pH for 20–30 min before each experiment. In addition, all experiments showed a constant slope (all $R^2 > 0.90$) with intercept values near zero (±10% of the total amount of calcium titrant added for that experiment). Examples of this metastability and constant slope have been provided in the Supplementary Material.

### 2.3. Analytical methods

After each experiment, samples were double filtered to determine the amount of solids precipitated. The filters were pre-rinsed with 500 mL of DI and 20 mL of sample to ensure that the filters did not contaminate the samples. First, the experimental solution was filtered using Whatman™ 934-AH RTU 1.5 μm glass microfiber filters. Following this, the experimental solution was filtered again using 0.2 μm SUPOR® 200 (Pall Corporation) filters. Both filters were weighed prior to filtration and then dried for 1 h at 103–105 °C before being placed in a desiccator to cool for at least 24 h. They were then weighed using a Mettler Toledo AE 160 balance to determine the amount of solids precipitated. Precipitated solids were analyzed using a Rigaku Ultima IV X-ray diffractometer (XRD) to verify the mineral phases present.

Filtered experimental solutions were analyzed for: (1) total phosphorus (TP) following United States Environmental Protection Agency (USEPA) Method 365.1 (USEPA, 1993) and (2) Ca using method USEPA 200.7 (USEPA, 1994) at the University of Florida Analytical Research Laboratory. Samples for TP analysis were preserved with sulfuric acid to pH < 2, and samples for Ca were preserved using nitric acid to pH < 3. Triplicate P samples for each experimental time shown in Table 1 had an average coefficient of variation of 0.15 (range: 0–0.57) for experiments at a pH of 8.5 and 0.09 (range: 0.01–0.40) for experiments at a pH of 9.5. Ca concentrations for all experiments were within ±10% of the target concentration of 100 mg $L^{-1}$. All samples were analyzed for DOC using a Shimadzu TOC-$V_{CPH}$ total organic carbon analyzer, and $UV_{254}$ using a Hitachi U-2900 spectrophotometer as described in Apell and Boyer (2010). All standard checks were within 10% of known values for P, Ca, and DOC measurements. Analytical replicates of both samples and standards were also within 10% for all measurements. Visual MINTEQ version 3.0 was used to calculate solution speciation.

## 3. Results and discussion

### 3.1. Calcium phosphorus co-precipitation

Experiments were conducted at different time intervals to determine P co-precipitation rates with Ca. Fig. 1 shows Ca and P precipitation rates for all experiments in this study. An analysis of the change in P concentration across time for each experimental solution showed that P precipitation was best modeled using first-order kinetics (see Supplementary Material). As a result, the average P precipitation rates for each experimental solution are presented in Fig. 1, normalized for the calcite seed area.

There was a lower change in P concentration as experimental time increased. This lower P removal is the result of two factors: (1) the lower phosphate activity in solution as a result of P precipitation (Sø et al., 2011) and (2) the saturation of active crystal growth sites with P. House and Donaldson (1986) and Dove and Hochella (1993) both showed that P can be incorporated into active crystal growth sites. However, House and Donaldson (1986) also showed that P can adsorb to other locations on the calcite surface. The total amount of adsorption sites, both active crystal growth sites and surface adsorption sites, are limited by the total area of the calcite seed (House and Donaldson, 1986; Sø et al., 2011). Consequently, as the experimental time increases, P precipitation rates decrease because adsorption sites become saturated with P.

Fig. 1 clearly shows that higher initial P concentrations do lead to higher P co-precipitation rates. P precipitation rates are higher at higher initial P concentrations because there is more P available for co-precipitation with Ca. Fig. 1 also shows that Ca precipitation is lower at increased initial P concentrations. Lin and Singer (2006) found the same trend of lower Ca precipitation rates in the presence of higher P. Higher P concentrations lead to more free hydrogen phosphate and phosphate, which replace water molecules on the calcite surface and can block active crystal growth sites leading to lower Ca precipitation rates (House and Donaldson, 1986).

The maximum surface density of co-precipitated P on the precipitated calcite surface can be calculated using the following equations (House and Donaldson, 1986; House, 1990; Hartley et al., 1997):

$$K_1 = 0.6915 \exp\left[\frac{E_a}{RT}\right] \tag{2}$$

$$K_2 = 4.361 \times 10^{-9} \exp\left[\frac{E_a}{RT}\right] \tag{3}$$

$$h(\mathrm{sol}) = \frac{K_1 a_{PO_4^{3-}} + K_2 a_{HPO_4^{2-}}}{1 + K_1 a_{PO_4^{3-}} + K_2 a_{HPO_4^{2-}}} \tag{4}$$

$$r = \frac{M_p}{M_S} \tag{5}$$

$$I(t) = \int_o^t h(\mathrm{sol}) \frac{1}{(1+r)^{2/3}} dn_{Ca_T} \tag{6}$$

$$\Delta n_{P_T} = \sigma N_A \delta I(t) \tag{7}$$

where $E_a$ is 18.2 kJ $mol^{-1}$ for $K_1$ and 42.6 kJ $mol^{-1}$ for $K_2$; $T$ is temperature (K); $R$ is the ideal gas constant (J $mol^{-1}$ $K^{-1}$); $a_{PO_4^{3-}}$ and $a_{HPO_4^{2-}}$ are the activities of phosphate and hydrogen phosphate in mol $L^{-1}$; $h(\mathrm{sol})$ is a function that describes the form of the absorption isotherm (House, 1990; Hartley et al., 1997); $r$ is the ratio of $M_p$, the amount of calcium precipitated (mg), to $M_s$, the mass of the calcite seed (mg); $dn_{Ca_T}$ is the change in calcium concentration (mmol $min^{-1}$); $t$ is time (min); $\Delta n_{P_T}$ is the change in P (μmol); $N_A$ is Avogadro's constant (molecules $mmol^{-1}$); $\delta$ is the molecular area of calcite on the surface ($20.1 \times 10^{-20}$ $m^2$-molecule$^{-1}$); and $\sigma$ is the maximum density of co-precipitated P (μmol $m^{-2}$).

Fig. 1 shows the $\sigma$ values for all experiments in this study. It is evident higher P concentrations lead to high P densities on the precipitated calcite surface, when comparing different P concentrations at the same pH and DOC. This suggests that while increasing P may result in lower Ca precipitation rates, P densities on the precipitated solids are actually higher with increased P.

Ca and P precipitation rates both play a role in the total amount of P precipitated during Ca–P co-precipitation. However, initial P concentration is also an important determining factor in the total amount of P removed through Ca–P co-precipitation. The more P available in solution at the start of an experiment, the higher the density of P on the calcite surface.

### 3.2. Calcium phosphorus co-precipitation rates as a function of pH and DOC

Fig. 1 shows Ca precipitation rates for experiments conducted at different pH and DOC levels. The figure clearly demonstrates that changes in pH and DOC all have an effect on the rate of both Ca and P precipitation. Higher pH values cause increased Ca precipitation because calcite becomes more saturated as pH increases. The degree of supersaturation for experiments conducted at a pH of 8.5 was 6.7, however, it substantially increased to 44.6 for experiments conducted at a pH of 9.5. In fact, no experiments were conducted without DOC at a pH of 9.5 because of the high degree of supersaturation. In the absence of DOC, the pH-stat system was unable to maintain the set pH value because of the high rate of Ca precipitation. This higher rate of Ca precipitation creates more active crystal growth sites and overall calcite surface area for P precipitation. As a result, there is increased P co-precipitation with calcite at pH 9.5. In addition, higher pH values cause an increase in the activity of deprotonated phosphate, which can also increase P precipitation. (Sø et al., 2011).

Previous work has shown that DOC has an inhibitory effect on pure Ca precipitation (as calcite) (Hoch et al., 2000; Lin et al., 2005). The results in Fig. 1 show that as DOC increases, Ca precipitation rates decline. At a pH of 8.5, Ca precipitation effectively ceases with the addition of 0.5 mg C $L^{-1}$ DOC. However, at a higher pH of 9.5, calcite is supersaturated enough to precipitate even in the presence of DOC. The precipitation rates for Ca at a DOC level of 2.5 mg C $L^{-1}$ at a pH of 9.5 are 10.8 and 8.2 times higher than the precipitation rates with no DOC at a pH of 8.5 for P levels of 100 μg P $L^{-1}$ and 50 μg P $L^{-1}$, respectively.

For experiments where the pH was held constant at a pH of 9.5, DOC levels also have a significant effect on the Ca precipitation rate. For example, Ca precipitation is 4.9 times higher at a DOC of 2.5 mg C $L^{-1}$ compared to 7.5 mg C $L^{-1}$ when P is held constant at 100 μg P $L^{-1}$. And when P is held constant at 50 μg P $L^{-1}$, Ca precipitation rates at a DOC of 2.5 mg C $L^{-1}$ are 3.6 and 11.4 times higher than those at DOC values of 7.5 mg C $L^{-1}$ and 15 mg C $L^{-1}$, respectively. While higher DOC levels do significantly decrease Ca precipitation rates at pH 9.5, Ca precipitation still occurs at DOC levels as high as 15 mg C $L^{-1}$.

DOC levels also have an effect on P precipitation rates. At a pH of 9.5 and a P concentration of 50 μg P/L, P precipitation rates are 3.4 times higher at DOC levels of 2.5 mg C $L^{-1}$ compared to 7.5 mg C $L^{-1}$ and 1.8 times higher at a DOC of 7.5 mg C $L^{-1}$ compared to 15 mg C $L^{-1}$. P precipitation rates are inhibited by increasing DOC concentrations due to the deprotonation of DOM carboxyl, and to a lesser extent phenolic, functional groups at the experimental pH values. As a result of deprotonation, DOC carries an overall negative charge and actively competes with P for adsorption sites on the calcite. However, it should be noted that the density of co-precipitated P, σ, on the calcite surface actually increases with higher DOC levels (see Fig. 1). This suggests that DOC slows the rate of Ca precipitation to a greater extent than P precipitation. As a result, increasing DOC levels mean more P precipitated with Ca. The size of DOC molecules likely limits their ability to bind to all available adsorption sites on the calcite surface, and as a result P is still able to precipitate in the presence of such high DOC levels. Changes in $SUVA_{254}$ data for experimental solution 12 support his conclusion. The initial $SUVA_{254}$ value for experimental solution 12 was 4.9 (L/mg $C^{-1}$ $m^{-1}$) and the final value was 4.2 (L/mg $C^{-1}$ $m^{-1}$). Since $SUVA_{254}$ is strongly correlated with the aromatic carbon content and molecular weight of DOC (Leenheer and Croue, 2003; Weishaar et al., 2003), the lower final $SUVA_{254}$ value suggests the preferential complexation of high molecular weight DOC and/or aromatic-rich DOC with the calcite surface. This conclusion is supported by the work of Inskeep and Bloom (1986), who showed that larger aromatic carboxylic acids are the primary cause of DOC inhibition of Ca precipitation.

Fig. 2 shows that a portion of DOC is lost from solution during Ca–P co-precipitation at pH 9.5. This effect is especially noticeable at higher DOC levels (15 mg C $L^{-1}$) because there is more DOC available to complex with the calcite in solution. Lin et al. (2005) showed that DOC can complex with free $Ca^{2+}$ in solution forming DOC–$Ca^{+}$ complexes, and these complexes can then react with the calcite surface inhibiting Ca precipitation. However, the results shown in Fig. 2 suggest that at pH 9.5, these DOC–$Ca^{+}$ complexes co-precipitate with calcite. Ca precipitation likely proceeds even in the presence of DOC–$Ca^{+}$ complexes because of the high degree of supersaturation for calcite, which overcomes the inhibitory effect of DOC. This incorporation of DOC–$Ca^{+}$ complexes into the precipitated solids explains the loss of DOC shown in Fig. 2. This conclusion is further supported by results shown in Section 3.3.

The lack of repeatability for experimental solution 11 is likely due to the high concentration of DOC and P in the water matrix. House and Donaldson (1986) showed that the amount of P adsorbed on the calcite surface could vary from experiment to experiment. It is also likely that the amount of DOC adsorbed on the calcite surface varies from experiment to experiment. Finally, there is variability in the type and amount of active sites on the

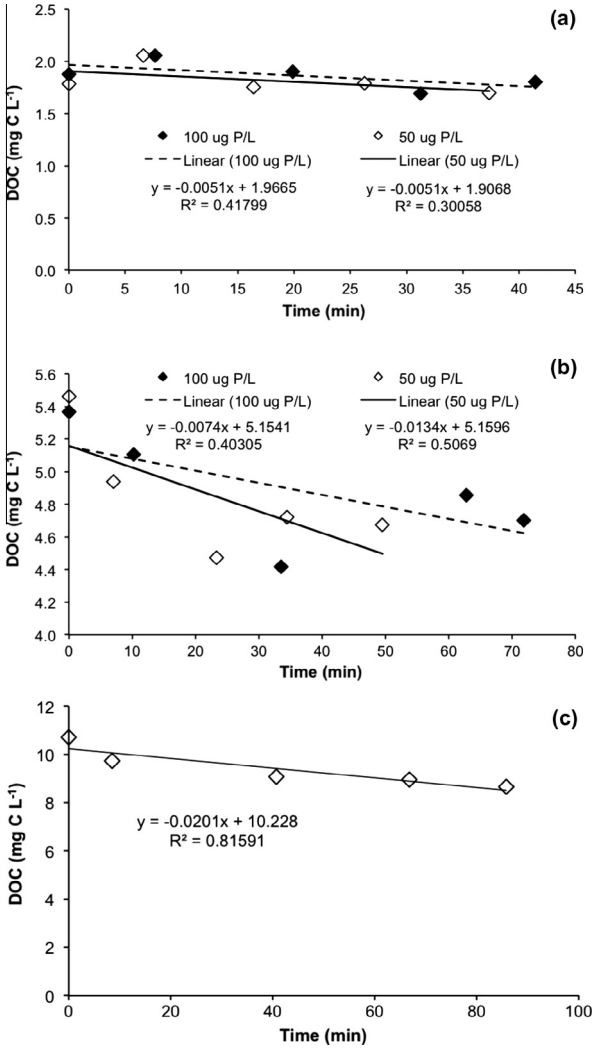


**Fig. 2.** Changes in DOC concentration for experiments conducted at pH 9.5 with: (a) P concentrations of 50 μg P $L^{-1}$ and 100 μg P $L^{-1}$ at an initial DOC of 2.5 mg C $L^{-1}$, (b) P concentrations of 50 μg P $L^{-1}$ and 100 μg P $L^{-1}$ at an initial DOC of 7.5 mg C $L^{-1}$ and (c) a P concentration of 50 μg P $L^{-1}$ at an initial DOC of 15 mg C $L^{-1}$.

calcite surface (Sø et al., 2011). The variability in both active crystal growth sites and the amount of P and DOC adsorption on the calcite surface made it infeasible to calculate P, Ca, and DOC precipitation rates for experimental solution 11.

### 3.3. Analysis of precipitated solids

Table 2 shows the Ca precipitation rate based on the collection and weighing of precipitated solids. The Ca precipitation rates calculated from precipitated solids are, on average, 13% less than the Ca precipitation rates calculated from the amount of titrant added to the pH stat system. These results confirm that the pH-stat system is accurately measuring the precipitation of Ca. The difference between the solid measurements and those from the pH-stat system are likely a result of two major factors: (1) inability to recover all the precipitated solids and (2) the initial complexation of free $Ca^{2+}$ ions with other anions in solution.

While all solid samples were double filtered according to the procedure outline in Section 2.3, there were likely some colloidal solids that passed through the 0.2 μm filter and remained in solution. These solids may have settled out prior to Ca analysis, and were not accurately measured, or they may have never been recovered from the reaction vessel. In addition, a Visual MINTEQ simulation of the experimental solution noted that up to 9% of the calcium is solution was complexed as $CaNO_3^+$. The Visual MINTEQ results suggest that when the experimental solution was prepared, initially, some of the free $Ca^{2+}$ complexed with the free nitrate in solution from the potassium nitrate added to adjust the ionic strength to 0.1 M. The Ca concentration of control samples, which were never used in the pH-stat system, support this conclusion. The Ca values for all control samples averaged 92 mg $L^{-1}$, while all other samples averaged 99.8 mg $L^{-1}$. This difference suggests that the initial Ca added to the pH-stat reactor simply restores the Ca concentration to the desired supersaturation level of 100 mg $L^{-1}$, but little to no precipitation is actually occurring. This conclusion is also supported by the results from experimental solutions 3–6 where there was little increase in solid Ca, however there was a measurable amount of Ca titrant added to the reactor.

Fig. 3 shows an XRD pattern for experimental solution 12. This pattern and other patterns from experimental solutions 1–10 (not shown) were an exact match for the mineral calcite, which was the solid mineral added to the pH-stat reactor to initiate Ca–P co-precipitation. Results from Figs. 1 and 2 show that there is precipitation of both P and DOC. However, the relative precipitation amount of both of these is low compared to Ca. As a result, there is not enough P or DOC to detect any other solid phases during XRD analysis.

While Fig. 3 demonstrates that calcite is the primary mineral precipitated during our experiments, Fig. 4 shows that the amount

**Table 2**
Ca and P precipitation rates for all experiments.

| Synthetic water number | Ca precipitation rate – pH-stat (μmol $s^{-1}$ $m^{-2}$)[a] | Ca precipitation rate – solids (μmol $s^{-1}$ $m^{-2}$)[a] |
|---|---|---|
| 1 | 1.40 | 1.23 |
| 2 | 2.38 | 2.04 |
| 3 | 0.10 | 0.00 |
| 4 | 0.22 | 0.09 |
| 5 | 0.11 | 0.00 |
| 6 | 0.10 | 0.00 |
| 7 | 15.07 | 13.00 |
| 8 | 19.47 | 16.62 |
| 9 | 3.10 | 2.78 |
| 10 | 5.35 | 4.87 |
| 11 | [b] | [b] |
| 12 | 1.71 | 1.47 |

[a] Normalized to the calcite seed area.
[b] No data, see Section 2.2.

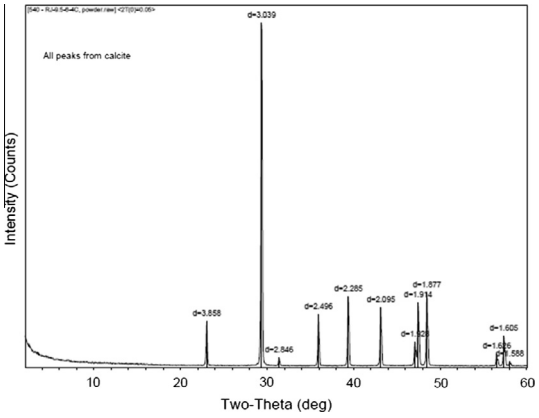


**Fig. 3.** XRD pattern for synthetic water 12. The pattern shown in an exact match for the mineral calcite.

of DOC precipitated is high enough to cause visible color differences between experiments with and without DOC. This color difference supports the conclusions in Section 3.2 that DOC forms DOC–$Ca^+$ complexes that are actively included in the calcite mineral precipitate in experimental solutions 7–10 and 12.

### 3.4. Implications for natural and engineered systems

Results from this research clearly show that DOC has an inhibitory effect on the co-precipitation of Ca and P at both pH 8.5 and 9.5. This finding is critical for engineered systems, where P, Ca, and DOC interact. For example, this information can be used to help determine target pH values for lime softening, if influent DOC and P concentrations are known. These results can also be used to predict the DOC and P removal effectiveness of lime softening. In corrosion control, these results can help predict how much calcite or Ca–P scale may form in the distribution system given a certain effluent DOC concentration. Knowing the amount of potential Ca–P scale formation will allow water utilities to assess the corrosion potential of their distribution systems.

Ca–P co-precipitation is also a vital P removal mechanism in many natural systems (Dierberg et al., 2002; Dodds, 2003; Knight et al., 2003; DeBusk et al., 2004; White et al., 2006; Mitsch and Gosselink, 2007). This research and other studies have shown that DOC concentrations as low as 0.5 mg C $L^{-1}$ can significantly decrease Ca precipitation at pH 8.5 (Hoch et al., 2000; Lin et al., 2005). However, DOC levels in many natural systems with Ca–P co-precipitation, such as the Florida Everglades, can approach

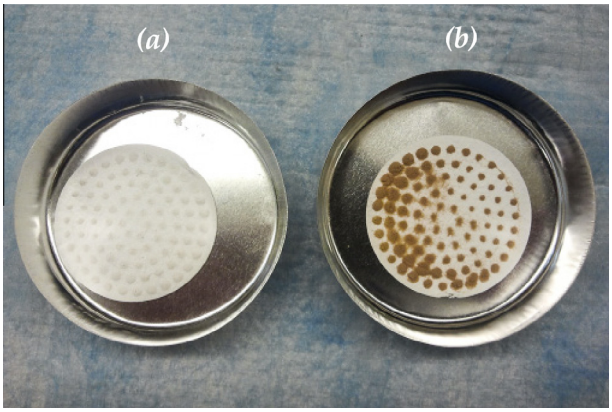


**Fig. 4.** Precipitated solids from experiments at: (a) a pH of 8.5 and 2.5 mg C $L^{-1}$ DOC and (b) a pH of 9.5 and 2.5 mg C $L^{-1}$ DOC. No Ca precipitation occurred in (a) because of the inhibitory effect of DOC.

15 mg C $L^{-1}$ or higher. In addition, the pH of the bulk water in these systems never approaches values greater than 8.5. There must be a plausible explanation for the occurrence of Ca–P co-precipitation in these systems with high DOC values.

The results presented in this article show that Ca–P co-precipitation occurs at pH 9.5 for DOC values as high as 15 mg C $L^{-1}$, and Hartley et al. (1996) showed that pH values at the surface of algal biofilms can reach values as high as 9.5, even when the pH of the bulk solution 2.15 mm above the biofilm is as low as 8. This research combined with the results of Hartley et al. (1996) suggest that Ca–P co-precipitation in high DOC natural systems likely occurs near the surface of algal biofilms or aquatic plants, where the pH can be significantly higher than the bulk water. This increased pH significantly increases the degree of supersaturation with respect to calcite, allowing Ca–P co-precipitation to proceed in the presence of high concentrations of potential inhibitors, such as DOC.

## 4. Conclusions

- Overall, DOC had a significant effect on the precipitation of Ca, which in turn affected the potential for P co-precipitation. At a pH of 8.5, the addition of 0.5 mg C $L^{-1}$ DOC effectively stopped Ca–P co-precipitation. However, raising the pH from 8.5 to 9.5 significantly increased the supersaturation of calcite and made Ca–P co-precipitation possible in the presence of DOC levels as high as 15 mg C $L^{-1}$.
- Higher P concentrations in solution lead to lower Ca precipitation rates because P acted as an inhibitor for Ca precipitation. P co-precipitation rates with Ca follow first-order kinetics, and P precipitation rates were higher at higher initial P concentrations.
- The density of co-precipitated P on the calcite surface was higher for experiments with higher initial P concentrations.
- DOC precipitated with Ca and P for experiments conducted at a pH of 9.5. DOC likely formed DOC–$Ca^{+}$ complexes that were incorporated into the precipitating calcite solid.
- Aromatic portions of the DOC preferentially inhibited the precipitation of Ca. The large molecular size of these fractions of DOC made them unable to bind to all available sites on the calcite seed, which allowed P to occupy open binding sites.
- Water treatment utilities can use the information provided about the inhibitory effect of DOC on Ca–P precipitation to help improve both lime softening and corrosion control processes.
- Ca–P co-precipitation is an important P removal mechanism in many natural systems. Previous research suggest that Ca–P co-precipitation in these systems occurs on the surface of photosynthesizing algal biofilms and submerged aquatic vegetation, where pH can be as high as 9.5. This previous research, when combined with results from this study that show that Ca–P co-precipitation is possible in the presence of high NOM (>5 mg C $L^{-1}$) at pH values of 9.5, explains how Ca–P co-precipitation occurs in these natural systems with high DOC (>5 mg C $L^{-1}$) and bulk water pH values of 8–8.5.

## Acknowledgements

The authors extend their gratitude to Ashley Walsh for her assistance running experiments. The authors also wish to thank other members of the research group for assisting with sample analysis. The article was improved by the insightful comments of anonymous reviewers. This work was supported in part by the Everglades Foundation and the USGS WRRI Project ID 2011FL267B. The Everglades Foundation and the USGS have not officially endorsed this publication and the views expressed herein may not reflect the views of the Everglades Foundation or the USGS.

## Appendix A. Supplementary material

Supplementary data associated with this article can be found, in the online version, at http://dx.doi.org/10.1016/j.chemosphere.2015.05.008.

## References

Apell, J.N., Boyer, T.H., 2010. Combined ion exchange treatment for removal of dissolved organic matter and hardness. Water Res. 44, 2419–2430.
Brunauer, S., Emmet, P.H., Teller, E., 1938. Adsorption of gases in multimolecular layers. J. Am. Chem. Soc. 60, 309–319.
Dartmann, J., Alex, T., Dorsch, T., Schevalje, E., Johannsen, K., 2004. Influence of decarbonisation and phosphate dosage on copper corrosion in drinking water systems. Acta Hydrochim. Hydrobiol. 32, 25–32.
Debusk, T., Grace, K., Dierberg, F., Jackson, S., Chimney, M., Gu, B., 2004. An investigation of the limits of phosphorus removal in wetlands: a mesocosm study of a shallow periphyton-dominated treatment system. Ecol. Eng. 23, 1–14.
Diaz, O., Reddy, K., Moore Jr., P.A., 1994. Solubility of inorganic phosphorus in stream water as influenced by pH and calcium concentration. Water Res. 28, 1755–1763.
Dierberg, F., Debusk, T., Jackson, S., Chimney, M., Pietro, K., 2002. Submerged aquatic vegetation-based treatment wetlands for removing phosphorus from agricultural runoff: response to hydraulic and nutrient loading. Water Res. 36 (6), 1409–1422.
Dodds, W., 2003. The role of periphyton in phosphorus retention in shallow freshwater aquatic systems. J. Phycol. 39 (5), 840–849.
Dove, P.M., Hochella, M.F., 1993. Calcite precipitation mechanisms and inhibitions by orthophosphate: in situ observations by scanning force microscopy. Geochim. Cosmochim. Acta 57, 705–714.
Hartley, A., House, W., Leadbeater, B., Callow, M., 1996. The use of microelectrodes to study the precipitation of calcite upon algal biofilms. J. Colloid Interface Sci. 183, 498–505.
Hartley, A., House, W., Callow, M., Leadbeater, B., 1997. Coprecipitation of phosphate with calcite in the presence of photosynthesizing green algae. Water Res. 31, 2261–2268.
Hoch, A., Reddy, M., Aiken, G., 2000. Calcite crystal growth inhibition by humic substances with emphasis on hydrophobic acids from the Florida Everglades. Geochim. Cosmochim. Acta 64, 61–72.
House, W., 1990. The prediction of phosphate coprecipitation with calcite in freshwaters. Water Res. 24, 1017–1023.
House, W., Donaldson, L., 1986. Adsorption and coprecipitation of phosphate on calcite. J. Colloid Interface Sci. 112, 309–324.
Inskeep, W., Bloom, P., 1986. Kinetics of calcite precipitation in the presence of water-soluble organic ligands. Soil Sci. Soc. Am. J. 50, 1167–1172.
Knight, R., Gu, B., Clarke, R., Newman, J., 2003. Long-term phosphorus removal in Florida aquatic systems dominated by submerged aquatic vegetation. Ecol. Eng. 20, 45–63.
Lauderdale, C., Chadik, P., Kirisits, M., Brown, J., 2012. Engineered biofiltration: enhanced biofilter performance through nutrient and peroxide addition. J. Am. Water Works Assoc. 104, E298–E309.
Leenheer, J., Croue, J., 2003. Characterizing aquatic dissolved organic matter. Environ. Sci. Technol. 37, 18A–26A.
Lin, Y.P., Singer, P.C., 2006. Inhibition of calcite precipitation by orthophosphate: speciation and thermodynamic considerations. Geochim. Cosmochim. Acta 70, 2530–2539.
Lin, Y., Singer, P., Aiken, G., 2005. Inhibition of calcite precipitation by natural organic material: kinetics, mechanism, and thermodynamics. Environ. Sci. Technol. 39, 6420–6428.
Mitsch, W.J., Gosselink, J.G., 2007. Wetlands. John Wiley & Sons, Inc., Hoboken, New Jersey.
Sø, H.U., Postma, D., Jakobsen, R., Larsen, F., 2011. Sorption of phosphate onto calcite; results from batch experiments and surface complexation modeling. Geochim. Cosmochim. Acta 75, 2911–2923.
Tomson, M., Nancollas, G., 1978. Mineralization kinetics: a constant composition approach. Science 200, 1059–1060.
United States Environmental Protection Agency (USEPA), 1993. Method 365.1: Determination of Phosphorus by Semi-Automated Colorimetry.
United States Environmental Protection Agency (USEPA), 1994. Method 200.7: Determination of Metals and Trace Elements in Water and Wastes by Inductively Coupled Plasma-Atomic Emission Spectroscopy.
Weishaar, J.L., Aiken, G.R., Bergamaschi, B.A., Fram, M.S., Fujii, R., Mopper, K., 2003. Evaluation of specific ultraviolet absorbance as an indicator of the chemical composition and reactivity of dissolved organic carbon. Environ. Sci. Technol. 37, 4702–4708.
White, J.R., Reddy, K.R., Majer-Newman, J., 2006. Hydrologic and vegetation effects on water column phosphorus in wetland mesocosms. Soil Sci. Soc. Am. J. 70, 1242–1251.